CrossMark
← click for updates

Steady shearing flows of deformable, inelastic spheres

Diego Berzi*[a] and James T. Jenkins[b]

We extend models for granular flows based on the kinetic theory beyond the critical volume fraction at which a rate-independent contribution to the stresses develops. This involves the incorporation of a measure of the duration of the particle interaction before and after this volume fraction. At volume fractions less than the critical, the stress components contain contributions from momentum exchanged in collisions that are influenced by the particle elasticity. At volume fractions greater than the critical, the stress components contain both static contributions from particle elasticity and dynamic contributions from the momentum transfer associated with the release of elastic energy by the breaking of force chains. A simple expression for the duration of a collision before and after the critical volume fraction permits a smooth transition between the two regimes and predictions for the components of the stress in steady, homogeneous shearing that are in good agreement with the results of numerical simulations. Application of the theory to steady, inhomogeneous flows reproduces the features of such flows seen in numerical simulations and physical experiments.

Introduction

Granular materials that are comprised of nearly spherical particles exhibit behaviour that ranges from that of a gas to that of a solid, depending on the nature of the interaction between the grains. These interactions depend upon the volume fraction of the solid, and the volume fraction is sensitive to the loading applied to the aggregate. The range of behaviours that granular materials exhibit parallels that seen in other systems of soft matter, such as colloids and non-Brownian suspensions.[1,2]

In shearing flows driven, for example, by the relative motion of two rigid, bumpy boundaries at volume fractions less than about 0.49, the spheres interact through collisions that can be regarded as instantaneous, binary, and uncorrelated. In this case, methods from the kinetic theory of dense gases that take into account the energy lost in a collision[3–5] can be used to predict the relationship between the forces necessary to maintain the flow and the rate of shearing. When the influence of the boundaries is negligible, both the pressure and the shear stress are quadratic in the shear rate; as a consequence, the strength of the velocity fluctuations, the analogue of the temperature, is quadratic in the shear rate. Because there is little scale separation in granular flows, there is no compelling reason why continuum descriptions should apply. However,

comparisons between predictions of continuum theories and the profiles of volume fraction, velocity, and temperature measured in physical experiments and discrete numerical simulations of steady flows show relatively good agreement[6–9] and this encourages their use.

Above a volume fraction of 0.49, at which a first-order phase transition between disordered and ordered states in an equilibrated system of colliding hard spheres is first possible,[10] molecular dynamics simulations show that correlations between collisions begin to influence the relationship between the components of the stress and the shear rate.[11–13] The introduction of an additional length scale in the relation for the rate of collisional dissipation of fluctuation energy associated with the size of clusters of interacting spheres modifies the stress relations in an appropriate way.[9,14–16] The length scale is determined by the competition between the orienting influence of the flow and the randomizing influence of the collisions, using a local balance between the rates of production and dissipation of fluctuation energy. This approach has been tested against discrete element simulations of steady flows in a variety of flow configurations.[17–20]

These extended stress relations apply until the mean separation distance between the edges of the spheres vanishes at least along the direction of principal compression, at which point, the stresses for hard spheres become singular.[20] The volume fraction at which this occurs is less than that for random close packing and is seen in numerical simulation to depend on the coefficient of sliding friction.[21] It can be interpreted as "the jamming transition" for shearing flows of compliant, frictional spheres.[1,22–25] However, discrete numerical simulations in two

[a] Department of Civil and Environmental Engineering, Politecnico di Milano, 20133 Milano, Italy. E-mail: diego.berzi@polimi.it

[b] School of Civil and Environmental Engineering, Cornell University, Ithaca, NY 14853, USA. E-mail: jtj2@cornell.edu

dimensions of the shearing of compliant, frictional, circular disks[26–28] indicate that there are three different jamming transitions. Consequently, more work is required in three dimensions to determine if, in fact, the volume fraction at which the stresses become singular is unique. We note that, because of the anisotropy inherent in a shearing flow, the critical volume fraction provides only a rough characterization of the singular state; descriptions of the anisotropy of this state are beginning to be developed.[29]

Replacing a rigid contact with a compliant contact has three consequences: it permits the introduction of a time associated with the duration of a collision before the hard-sphere singularity;[30] it relaxes the singularity of the stresses at this singularity; and it allows prediction of the stresses at volume fractions greater than that at the singularity. The stresses at volume fractions beyond the hard-sphere singularity have parts that depend on the shear rate and parts that depend on the deformation of the contact. We refer to these as the rate-dependent and rate-independent[31,32] parts of the stress.

In this paper, we calculate stress relations for steady, shearing flows of deformable, elastic spheres that apply at volume fractions less than, at, and greater than the hard-sphere singularity. We do this by extending the stress relations of kinetic theories to collisions with a finite duration and employing the elastic component of the contact to describe the stresses associated with enduring contact of the spheres.

We first focus on steady, homogeneous shearing flows and compare the predicted stresses with those measured in numerical simulations.[21,33,34] The predictions compare well over the range of volume fraction before and after the hard sphere singularity and over eleven orders of magnitude of the contact stiffness. The model requires no parameters other than the contact stiffness, coefficient of collisional restitution, and sliding friction of the spheres. An interesting result is that the viscosity below the singularity is seen to increase with the fluctuation energy, as in a dense gas, but to decrease with fluctuation energy above the singularity, as in a liquid. We also consider steady, inhomogeneous shearing flows, in which the conduction of fluctuation energy is important, and reproduce, for spheres, the qualitative feature of stress relations measured in discrete numerical simulations of circular disks.[35]

Theory

We consider a steady, uniform, unidirectional, shearing flow of spheres of mass density ρ_p and diameter d. Their interactions are characterized, in part, by a normal coefficient of restitution e and contact friction μ. We take ν to be the solid volume fraction, and x and y to be the flow and shear directions, respectively. Then, u is the only component of the mean velocity of the particles and u' is the shear rate, with the prime denoting a derivative with respect to y. We define the critical volume fraction, ν_c, as the volume fraction above which a rate-independent component of the stresses develops. At greater volume fractions, the mean distance between at least some sphere centres is less than one diameter – indicating persistent

deformations of such particles.[24] We distinguish between flows at volume fraction less than and greater than ν_c, referring to those at volume fractions less than ν_c as collisional and those above ν_c as deformational. We first carry out calculations for contact forces that are linear in the contact deformation and indicate the modifications for non-linear contacts. Also, for the sake of simplicity, we limit our analysis to dense flows; in these, the dependence of the coefficients of kinetic theory on the volume fraction is proportional to that of the radial distribution function at contact.

Collisional regime

In this regime, the stresses are due to the transfer of momentum in collisions, the mean separation distance between the centres of spheres is greater than one diameter, and the granular material behaves as a dense gas. Consequently, we begin with the stress relations of kinetic theory, extended to include an additional length scale in the rate of collisional dissipation,[14,15,18] and modify them to incorporate the deformation of a contact during a collision.[32] When the contact is compliant, the time interval between two successive collisions is equal to the time of free flight, t_f, plus the duration of the contact, t_c.

The time of free flight is $(\pi^{1/2}/24)d/(GT^{1/2})$, where G is the product of the volume fraction and the radial distribution function at collision and T is the one-third the mean-square of the velocity fluctuations – the granular temperature.[36] For the volume fraction dependence of the radial distribution function g_0 of two colliding spheres, we adopt the expression of Vescovi et al.,[19] which smoothly interpolates between the form due to Carnahan and Starling, appropriate at small volume fractions, and that which diverges at a critical volume fraction:[20]

$$g_0 = f\frac{2 - \nu}{2(1 - \nu)^3} + (1 - f)\frac{2}{\nu_c - \nu}, \tag{1}$$

where $f = (\nu_c + \nu - 0.8)(\nu_c - \nu)/(\nu_c - 0.4)^2$. For rigid contacts, shearing ceases at the critical volume fraction and the system is said to be jammed. For deformable contacts, discrete numerical simulations show that the value of the critical volume fraction depends only on the coefficient of friction.[21]

The duration of a collision is proportional to the ratio of the particle diameter to the elastic wave speed in the particle: $c = (E/\rho_p)^{1/2}$, where E the Young's modulus of the material of the spheres.[30] We take the coefficient in the proportion to be 1/5, which provides the best fitting with the simulations of simple shearing shown later. Consequently, the frequency of collisions – the inverse of the time interval between two successive collisions – is reduced for deformable particles with respect to that for rigid particles by the factor

$$\frac{t_f}{t_f + t_c} = \frac{\pi^{1/2}}{24}\frac{d}{GT^{1/2}}\left(\frac{\pi^{1/2}}{24}\frac{d}{GT^{1/2}} + \frac{d}{5c}\right)^{-1}$$

$$= \left[1 + \frac{24G}{5\pi^{1/2}}\left(\frac{\rho_p T}{E}\right)^{1/2}\right]^{-1}, \tag{2}$$

Because the collisional stresses, the collisional rate of dissipation of the fluctuation energy, and the flux of fluctuation energy

are all proportional to the frequency of collision, the constitutive relations of extended kinetic theory for rigid particles, a modification of those of Garzo and Dufty,[4] must be multiplied by the factor of eqn (1) when applied to deformable spheres.

The rigid and deformable contributions to the constitutive relation for the pressure p and the shear stress s are best seen when the inverses of these are written as the sums of the inverses of the two contributions:

$$p^{-1} = \left[2(1+e)G\rho_p\nu T\right]^{-1} + \left[\frac{5\pi^{1/2}\nu(1+e)}{12}(\rho_p ET)^{1/2}\right]^{-1}, \quad (3)$$

and

$$s^{-1} = \left(\frac{8JG}{5\pi^{1/2}}\rho_p\nu T^{1/2}d|u'|\right)^{-1} + \left[\frac{\nu J}{3}(\rho_p E)^{1/2}d|u'|\right]^{-1}, \quad (4)$$

respectively, where the dependence of J on the coefficient of restitution is given by $J = (1+e)/2 + \pi(1+e)^2(3e-1)/[96-24(1-e)^2-20(1-e^2)]$.[15] The first terms on the right-hand sides of eqn (3) and (4) are the inverses of the constitutive relations for rigid spheres; the second terms are the inertial-elastic contributions,[37] called the intermediate contributions by Chialvo et al.,[21] who explored shearing of deformable spheres in discrete numerical simulations. Unlike the fits by Chialvo et al. to the constitutive relations,[21] the expressions in eqn (3) and (4) depend also on the granular temperature; this permits the analysis of inhomogeneous shearing flows, such as those between rigid, bumpy boundaries,[38] in which the temperature is not proportional to the square of the shear rate.

A consequence of the extension of the frequency of collisions from rigid to deformable particles is that the pressure and the shear stress are no longer singular at $\nu = \nu_c$. For volume fractions close to the critical, G tends to infinity; hence, the first terms on the right hand side of eqn (3) and (4) vanish, while the other terms remain finite.

Similarly, the expressions of the rate of collisional dissipation of the fluctuation energy Γ is

$$\Gamma^{-1} = \left[\frac{12(1-\varepsilon^2)G}{\pi^{1/2}L}\rho_p\nu T^{3/2}\right]^{-1} + \left[\frac{5(1-\varepsilon^2)\nu}{2L}(\rho_p E)^{1/2}T\right]^{-1}, \quad (5)$$

where ε is an effective coefficient of restitution, which takes into account the additional dissipation of the fluctuation energy due to the rotation and contact friction of the particles.[39,40] In eqn (5), L is an additional length scale related to the correlation of collisions at volume fractions larger than 0.49.[14] It is determined by a balance between the ordering influence of the shearing and the randomizing influence of the collisions:

$$L = f_0 d \frac{u'd}{T^{1/2}}, \quad (6)$$

where discrete numerical simulations indicate that the coefficient f_0 is singular at random close packing:[20]

$$f_0 = \left[\frac{4J}{15(1-\varepsilon^2)}\right]^{1/2}\left[1 + \frac{26(1-\varepsilon)}{15}\frac{\max(\nu-0.49,0)}{0.64-\nu}\right]. \quad (7)$$

When the flow interacts with boundaries, there is a flux of fluctuation energy directed either into or out of the flow.[38,41,42] In such situations, the granular temperature must be determined as a solution of the differential equation that expresses the balance of fluctuation energy. The constitutive relation for the inverse of the flux of fluctuation energy Q for deformable spheres is

$$Q^{-1} = \left(-\frac{4MG}{\pi^{1/2}}\rho_p\nu dT^{1/2}T'\right)^{-1} + \left[-\frac{5\nu M}{6}(\rho_p E)^{1/2}dT'\right]^{-1} \quad (8)$$

where $M = (1+e)/2 + 9\pi(1+e)^2(2e-1)/[128-56(1-e)]$.[15] Here, we have ignored the contribution to the energy flux proportional to the gradient of the volume fraction,[4] which is negligible for dense flows.

Deformational regime

In this case, the mean separation distance, at least along the direction of the principal compression axis, is zero. Volume fractions larger than ν_c can be achieved in a disordered assembly of particles only if some particles deform. Therefore, an elastic component of the stresses associated with such persistent deformations develops. For isotropic compression of an isotropic aggregate, the elastic contribution to the pressure is proportional to the product of the normal component of the contact force P, the separation between the centres d, the number of contacts per sphere Z, and the number of spheres per unit volume $6\nu/(\pi d^3)$:[43]

$$p_e = \frac{P\nu Z}{\pi d^2}, \quad (9)$$

For linear contacts, P is related to the normal component of the contact displacement δ through the contact stiffness $\pi dE/4$:[33]

$$P = \frac{\pi}{4}dE\delta, \quad (10)$$

The contact displacement can be related to the volume fraction at a fixed coordination number by treating the particle deformations as overlapping. Then, the ratio of the total overlapped volume to the particle volume gives the increase in the volume fraction from the critical value,

$$\frac{\nu}{\nu_c} = 1 + \frac{Z2\pi\delta^2(d/2-\delta/3)}{\pi d^3/6} \simeq 1 + 6Z\left(\frac{\delta}{d}\right)^2, \quad (11)$$

in which we assume that the δ/d ratio is small. Then, with eqn (10), p_e is proportional to the square-root of the product of $(\nu - \nu_c)$ and Z. Discrete numerical simulations of simple shearing of frictional, deformable spheres[33] indicate that the coordination number is approximately linear in the increase of volume fraction from ν_c, with a slope of about ten, at least for the softest particles. With this, we find that the elastic pressure is roughly equal to the product of E and the excess of the volume fraction above the critical. On the basis of fitting with numerical simulations, we adopt the expression

$$p_e = 0.6\frac{\pi}{4}(\nu-\nu_c)E. \quad (12)$$

For stiffer particles, the coordination number scales with the square root of the increase of volume fraction from ν_c,[29,33] but

the pressure still increases linearly with the difference $\nu - \nu_c$ in steady, homogeneous shearing.[29] Consequently, we assume that eqn (12) holds for any value of the particle stiffness.

Shearing forces the individual particles to make and break chains of frictional contacts, sometimes violently,[44] so that a component of the stresses associated with the transfer of momentum is still present at $\nu > \nu_c$, with the frequency of transfer equal to the inverse of contact duration. We model this elastic-inertial pressure in the same way as we model the inertial-elastic pressure in the collisional regime. The total pressure is the sum of the elastic-inertial and the purely elastic components,

$$p = \frac{5\pi^{1/2}\nu(1+e)}{12}\left(\rho_p ET\right)^{1/2} + 0.6\frac{\pi}{4}(\nu - \nu_c)E. \qquad (13)$$

The first and second terms on the right hand side of eqn (13) can be identified with, respectively, the intermediate and quasi-static pressures of Chialvo et al.[21]

We take the constitutive relation for the elastic-inertial shear stress to be the inverse of the inertial-elastic contribution to eqn (4). Once again, the total shear stress is the sum of two components: the elastic-inertial and the purely elastic. In the steady state, both the purely elastic shear stress and the purely elastic pressure p_e are proportional to the stiffness, so they are proportional to each other. Hence, the total shear stress may be written as

$$s = \frac{\nu J}{3}\left(\rho_p E\right)^{1/2}d|u'| + \eta p_e. \qquad (14)$$

where η is the constant of proportionality. Discrete numerical simulations of unsteady, homogeneous shearing in the rate-independent regime,[29] indicate that the ratio of the purely elastic shear stress to the purely elastic pressure is proportional to the anisotropy of the contact network. Because the ratio of the elastic-inertial shear stress to the elastic-inertial pressure is sensitive to this anisotropy in the same way, we determine η from this ratio:

$$\eta = \frac{4J}{5\pi^{1/2}(1+e)}\frac{d|u'|}{T^{1/2}}. \qquad (15)$$

The values of η obtained from eqn (15) in simple shearing[20] with different particle friction coefficients are in agreement with the measurements of the constant stress ratio obtained in numerical simulations when $\nu > \nu_c$ and the particles are sufficiently rigid.[21]

Because of the energy released by the breaking of chains, the rate of dissipation of the fluctuation energy and the fluctuation energy flux also persist at volume fractions larger than the critical. We take the dissipation rate to be the inverse of the inertial-elastic contribution to eqn (5),

$$\Gamma = \frac{5\left(1-\varepsilon^2\right)\nu}{2L}\left(\rho_p E\right)^{1/2}T, \qquad (16)$$

and we assume that the correlation length is still given by eqn (6), with f_0 evaluated at $\nu = \nu_c$. Finally, we take the flux of fluctuation energy to be the inverse of the inertial-elastic contribution to eqn (8),

$$Q = -\frac{5\nu M}{6}\left(\rho_p E\right)^{1/2}dT'. \qquad (17)$$

Modifications for Hertzian contacts

Real spheres interact through Hertzian contacts. In this case, the duration of contact is[45]

$$t_c = 1.47\left(\frac{5\sqrt{\pi}}{4}\rho_p\frac{1-\psi^2}{E}\right)^{2/5}\frac{d}{(T/3)^{1/10}}, \qquad (18)$$

where ψ is Poisson's ratio, and we have assumed the pre-collisional velocity equal to $(T/3)^{1/2}$. Then, eqn (2) becomes

$$\frac{t_f}{t_f + t_c} = \left[1 + 1.47\frac{24G}{\pi^{1/2}}\left(\frac{3^{1/4}5\sqrt{\pi}}{4}\rho_p\frac{1-\psi^2}{E}T\right)^{2/5}\right]^{-1}. \qquad (19)$$

Using this, the derivation the constitutive relations for the inertial stresses, the rate of dissipation and the flux of fluctuation energy is straightforward.

For Hertzian spheres, the normal contact force is[43]

$$P = \frac{2}{9\sqrt{3}}\frac{Sd^2}{1-\psi}\left(\frac{6\delta}{d}\right)^{3/2}, \qquad (20)$$

where S is the shear modulus. Eqn (20) must be used instead of eqn (10) in eqn (9) to calculate the purely elastic pressure. If the relation between the volume fraction and the coordination number is approximately linear, we obtain

$$p_e \propto \frac{S}{1-\psi}(\nu - \nu_c), \qquad (21)$$

where the coefficient of proportionality is of order one. This dependence has been observed in the numerical simulations.[21]

Simple shearing

We next test the theory against numerical simulations of steady, homogeneous shearing of compliant, frictional spheres that interact through linear springs and dashpots in parallel.[21,33,34] In this case, Young's modulus is $E = 4k/(\pi d)$, where k is the stiffness of the normal spring.[33]

In simple shearing, the volume fraction and the granular temperature are uniform, so that the balance of fluctuation energy reduces to

$$(s - \eta p_e)|u'| = \Gamma, \qquad (22)$$

where we have assumed that the work of the purely elastic shear stress is completely recoverable and does not produce fluctuation energy.[31,32] This gives

$$\frac{T}{u'^2 d^2} = \frac{2J}{15(1-\varepsilon^2)}\left[1 + \frac{26(1-\varepsilon)}{15}\frac{\max(\nu - 0.49, 0)}{0.64 - \nu}\right], \qquad (23)$$

for volume fractions less than the critical, and

$$\frac{T}{u'^2 d^2} = \frac{2J}{15(1-\varepsilon^2)}\left[1 + \frac{26(1-\varepsilon)}{15}\frac{\nu_c - 0.49}{0.64 - \nu_c}\right], \qquad (24)$$
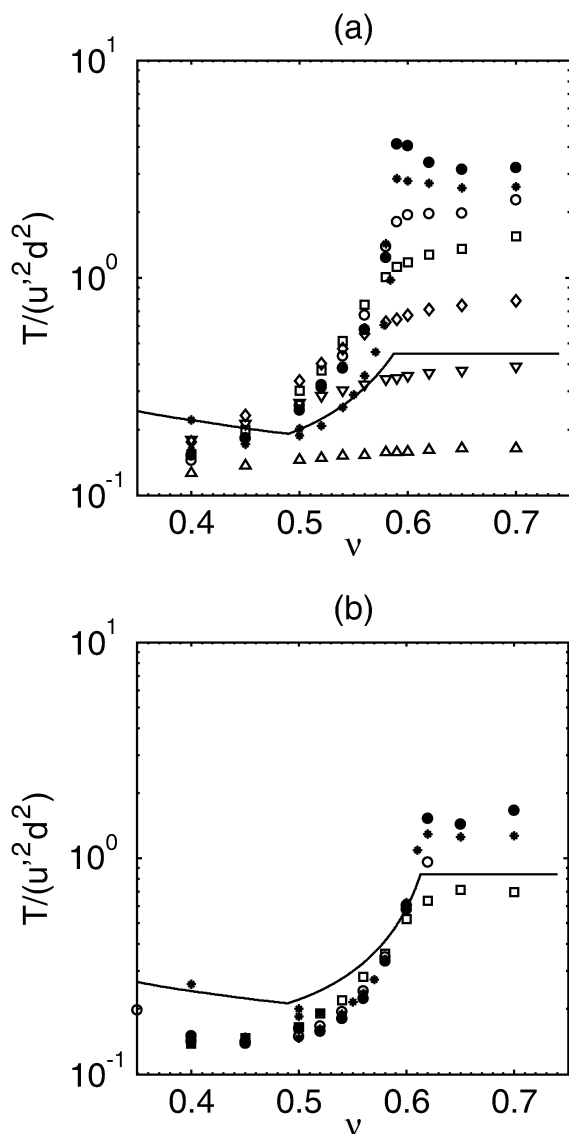
Fig. 1 Dimensionless granular temperature as a function of the volume fraction: predicted (lines) and measured by Ji and Shen[33] and Chialvo and Sundaresan[34] (symbols). Here, and in the following plots, the measured results are for dimensionless particle stiffness equal to: 10^1 (hollow upper triangles); 10^2 (hollow lower triangles); 10^3 (hollow diamonds); 10^4 (hollow squares); 10^5 (hollow circles); 10^6 (stars); 10^7 (solid circles); 10^8 (solid squares); 10^9 (solid diamonds); 10^{10} (solid lower triangles); 10^{11} (solid upper triangles).

for volume fractions larger than the critical. Eqn (23) and (24) imply that in simple shearing, the granular temperature, made dimensionless with the product of the particle diameter and the shear rate, is a function only of the volume fraction, and constant for $\nu > \nu_c$.

In Fig. 1a and b, we compare the predicted dimensionless granular temperature with the measurements in discrete numerical simulations of simple shearing: in Fig. 1a, when $e = 0.7$ and $\mu = 0.5$, so that $\nu_c = 0.587$ and $\varepsilon = 0.53$;[21,40] and, in Fig. 1b, when $e = 0.7$ and $\mu = 0.1$, so that $\nu_c = 0.613$ and $\varepsilon = 0.59$.[21,40] The numerical simulations have been performed for dimensionless particle stiffness $k/(\rho_p u'^2 d^3)$ ranging from 10 to 10^7.

The agreement is good when $\mu = 0.1$, and acceptable when $\mu = 0.5$, at least for volume fractions less than the critical value.

As anticipated, the dimensionless granular temperature is nearly constant beyond the transition, although its value increases with the dimensionless particle stiffness and seems to saturate, if the spheres are stiff enough. We associate the deviations from the numerical simulations with multiple interactions, which are not presently incorporated in the inertial parts of the constitutive relations.

We could certainly improve the agreement with the measurements by modifying the function f_0 in the correlation length, which has been accurately tested only against the results of numerical simulations of frictionless particles,[19] to incorporate the influence of the particle friction, and by modelling the role of multiple interactions, at least in the dissipation rate. We prefer to avoid those additional complications for several reasons. First, the agreement between the theory and the numerical results is less adequate when $\mu = 0.5$, $\nu > \nu_c$ and the particles are stiff. In that case, the elastic-inertial component is a small fraction of the total stress, so that a poor estimate of the granular temperature does not substantially affect the predictions of the pressure and the shear stress. Also, a friction coefficient of 0.5 is rather large; most real particles are characterized by friction coefficients closer to 0.1.[46] Finally, the measurements of Ji and Shen[33] differ from those of Chialvo and Sundaresan[34] for the same dimensionless stiffness of 10^6, indicating an uncertainty in the measurements. We postpone the refinement of the model to improve the prediction of the granular temperature for large friction and to include the role of multiple collisions to future work.

We can re-write the full constitutive relations for the pressure and the shear stress in dimensionless terms using the density and diameter of the spheres, the shear rate, and the particle stiffness instead of Young's modulus, making use of eqn (15):

$$\left(\frac{p}{\rho_p u'^2 d^2}\right)^{-1} = \left[2(1+e)\nu G \frac{T}{u'^2 d^2}\right]^{-1}$$

$$+ \left[\frac{5\pi^{1/2}\nu(1+e)}{12}\left(\frac{4}{\pi}\frac{T}{u'^2 d^2}\frac{k}{\rho_p u'^2 d^3}\right)^{1/2}\right]^{-1},$$

(25a)

if $\nu < \nu_c$, while

$$\frac{p}{\rho_p u'^2 d^2} = \frac{5\pi^{1/2}\nu(1+e)}{12}\left(\frac{4}{\pi}\frac{T}{u'^2 d^2}\frac{k}{\rho_p u'^2 d^3}\right)^{1/2}$$

$$+ 0.6(\nu - \nu_c)\frac{k}{\rho_p u'^2 d^3},$$

(25b)

if $\nu \geq \nu_c$; and

$$\left(\frac{s}{\rho_p u'^2 d^2}\right)^{-1} = \left[\frac{8J\nu G}{5\pi^{1/2}}\left(\frac{T}{u'^2 d^2}\right)^{1/2}\right]^{-1}$$

$$+ \left[\frac{\nu J}{3}\left(\frac{4}{\pi}\frac{k}{\rho_p u'^2 d^3}\right)^{1/2}\right]^{-1},$$

(26a)

if $\nu < \nu_c$, while

$$\frac{s}{\rho_p u'^2 d^2} = \frac{4J}{5\pi^{1/2}(1+e)}\left(\frac{T}{u'^2 d^2}\right)^{-1/2}\frac{p}{\rho_p u'^2 d^2}, \qquad (26b)$$

if $\nu \geq \nu_c$. In simple shearing, these are functions only of ν, through eqn (23) and (24), and the dimensionless stiffness.

Fig. 2a and b show the predicted dimensionless pressure and shear stress, compared with the results of numerical simulations of simple shearing,[21,33,34] for a range of dimensionless stiffness, $k/(\rho_p u'^2 d^3)$, from 10 to 10^{11} when $e = 0.7$ and $\mu = 0.5$.

Also shown are the curves for rigid particles, that is, for infinite k, for which the collisions are instantaneous and binary and no disordered assembly is possible beyond ν_c. The predictions agree well with the simulations. The volume fraction at
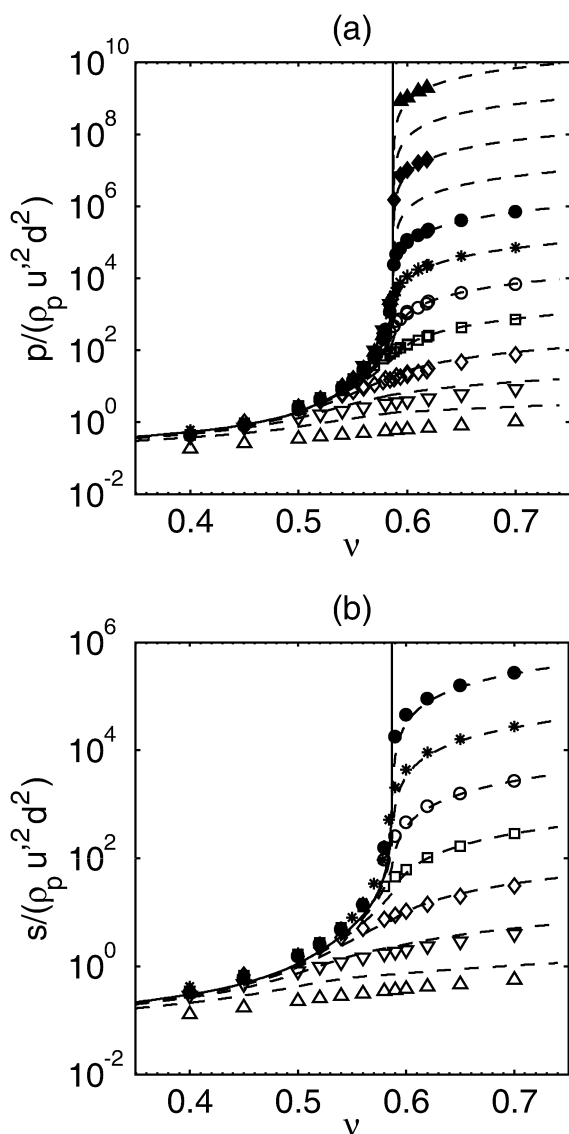

(a)

(b)

Fig. 2 Dimensionless (a) pressure and (b) shear stress as functions of the volume fraction as predicted (dotted lines) and measured by Ji and Shen,[33] Chialvo *et al.*,[21] and Chialvo and Sundaresan[34] (symbols), when $e = 0.7$ and $\mu = 0.5$. The symbols have the same significance as in Fig. 1. Also shown are the theoretical curves for perfectly rigid particles (solid lines).
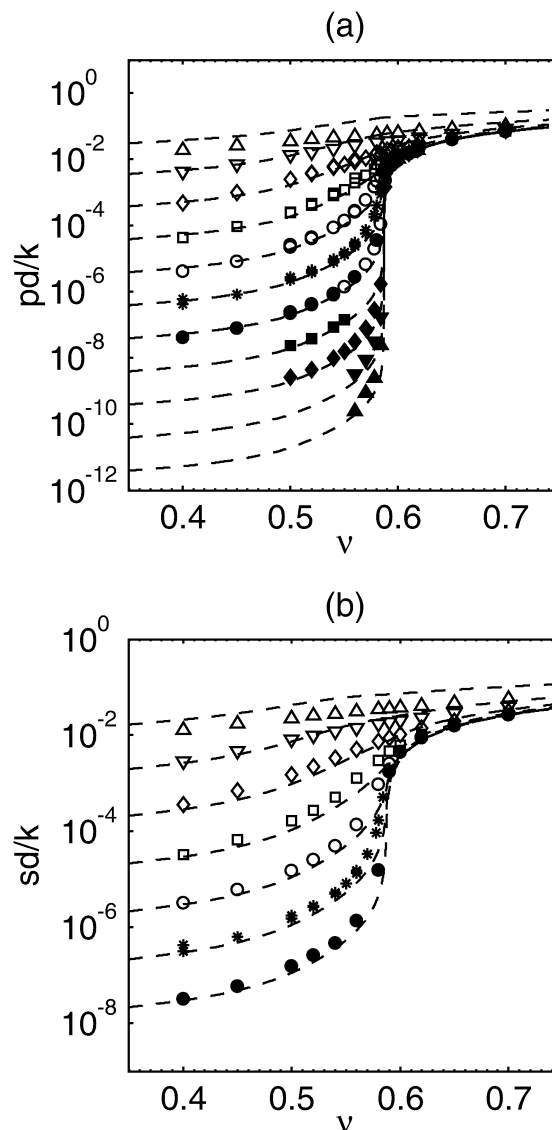

(a)

(b)

Fig. 3 (a) Pressure and (b) shear stress made dimensionless using the particle stiffness and diameter *versus* volume fraction as predicted (dotted lines) and measured by Ji and Shen,[33] Chialvo *et al.*,[21] and Chialvo and Sundaresan[34] (symbols) when $e = 0.7$ and $\mu = 0.5$. The symbols have the same significance as in Fig. 1.

which the data depart from the rigid curve increases with the particle stiffness. For real spheres, the collisions can be considered instantaneous and binary up to volume fractions close to the critical value.

If the stiffness and the particle diameter are used to scale the stresses, the results from the numerical simulations collapse at volume fractions larger than ν_c, where the purely elastic stresses dominate, as already observed by Ji and Shen.[33] The agreement between the predictions and the numerical simulations is again remarkable (Fig. 3).

Fig. 4 shows the comparison between the present theory, the constitutive relation for the pressure suggested by Chialvo *et al.*[21] through fitting with their simulations, and the measurements in discrete numerical simulations[21,33,34] when $e = 0.7$,
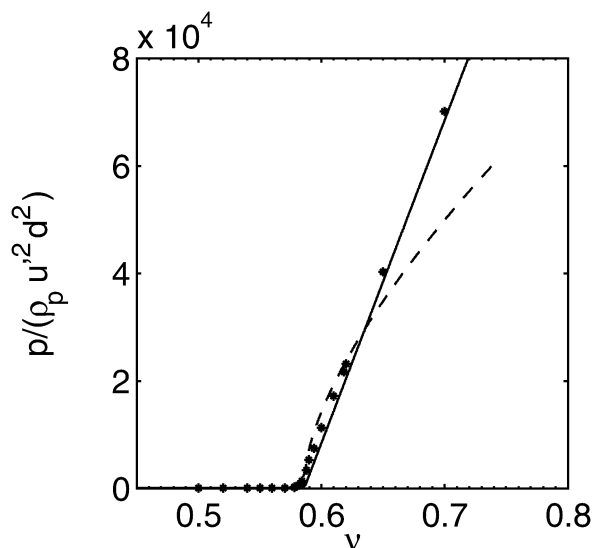
Fig. 4 Dimensionless pressure as a function of the volume fraction as predicted by the present model (solid line), the model of Chialvo *et al.*[21] (dotted line) and measured by Ji and Shen,[33] Chialvo *et al.*,[21] and Chialvo and Sundaresan[34] (symbols) when $e = 0.7$, $\mu = 0.5$ and $k/(\rho_p u'^2 d^3) = 10^6$.

$\mu = 0.5$, and the dimensionless stiffness is 10^6. The data tests the validity of the linear dependence of the purely elastic pressure on the volume fraction against the power law dependence with an exponent equal to 2/3 suggested by Chialvo *et al.*[21]

Fig. 5 shows the comparison between the predicted dimensionless pressure and shear stress and those measured in discrete numerical simulations by Chialvo *et al.*,[21] Chialvo and Sundaresan,[34] and Shen (personal communication) for various dimensionless stiffness, when $e = 0.7$ and $\mu = 0.1$.

Inhomogeneous shearing in the deformational regime

In inhomogeneous, steady flows, in which $\nu > \nu_c$, the shear rate is small and the production of fluctuation energy is negligible. In this case, the balance of fluctuation energy is, simply,

$$-\frac{dQ}{dy} = \Gamma, \tag{27}$$

where y is taken to increase in the direction of increase of the volume fraction. That is, the diffusion of the fluctuation energy balances its dissipation.[42] Using eqn (16) and (17), we obtain

$$\frac{d^2 T}{dy^2} = \frac{1}{\lambda^2} T, \tag{28}$$

where $\lambda^2 = dLM/[3(1 - \varepsilon^2)]$. Eqn (28) can be solved to determine the distribution of the granular temperature in the flow. As a first approximation, we take the correlation length L to be constant and equal to its value in simple shearing, determined using eqn (24) in eqn (6),

$$\frac{L}{d} = 1 + \frac{26(1 - \varepsilon)}{15} \frac{\nu_c - 0.49}{0.64 - \nu_c}. \tag{29}$$
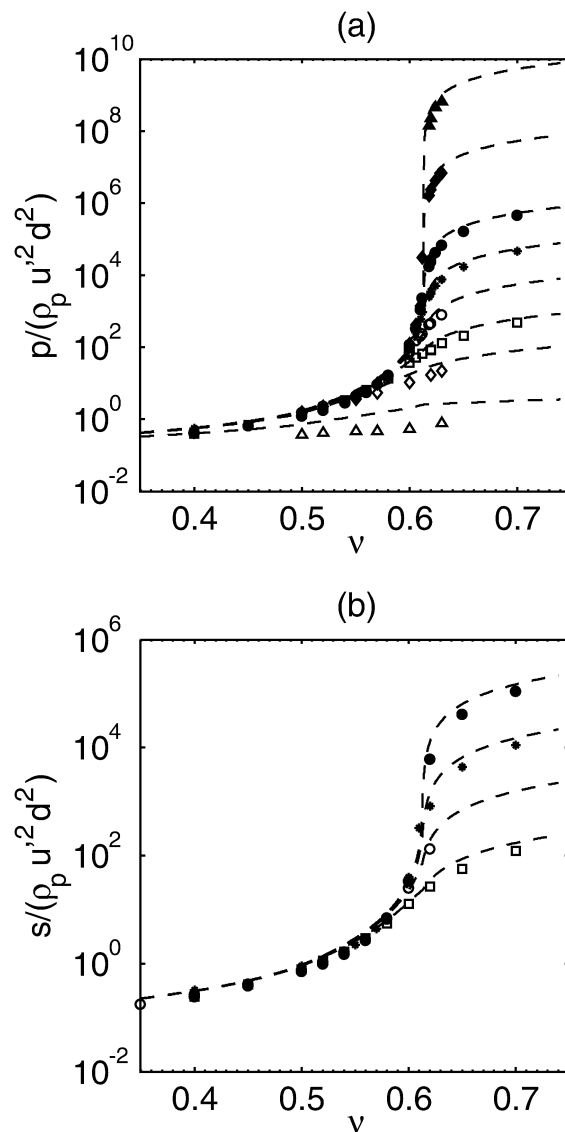

Fig. 5 Dimensionless pressure (a) and shear stress (b) as functions of the volume fraction as predicted (dotted lines) and measured by Chialvo *et al.*,[21] Chialvo and Sundaresan,[34] and Shen (personal communication) (symbols) when $e = 0.7$ and $\mu = 0.1$. The symbols have the same significance as in Fig. 1.

With this, λ is constant and the solution to eqn (28) is

$$T \propto \exp\left(-\frac{y}{\lambda}\right). \tag{30}$$

Creeping flow

Given the distribution of temperature, we seek to determine the velocity profile in the creeping bed below an inclined, collisional shearing flow that is driven by gravity.[47] There the stress ratio is given by eqn (15), and is proportional to the ratio of the shear rate to the square root of the granular temperature. If there are no sidewalls in such a flow, the ratio of the shear stress to the pressure is constant and equal to the tangent of the angle of inclination of the free surface. Then, the shear rate in the bed is directly proportional to the square root of the granular temperature and the velocity decays exponentially,

with a decay length equal to 2λ. For $e = 0.7$ and $\mu = 0.5$, the decay length of the velocity is roughly equal to two diameters, close to what is observed in the creeping flow of glass spheres.[47]

Annular shear flow

Another interesting flow is annular shearing. This was investigated by Koval et al.[35] in two-dimensional discrete element simulations of compliant, frictional, circular disks and modelled by Kamrin and Koval[48] using a second-order differential equations for the shear rate. Here, we focus on the three-dimensional case, in which spheres are sheared between two coaxial cylinders, with the gravity acting perpendicular to the plane of shearing. We solve for the flow field in a plane perpendicular to the axis of the cylinders. In doing this, we take R to be the radius of the inner cylinder, which is rotating at constant angular velocity, and $2R$ to be the radius of the outer cylinder, which is fixed, as in Koval et al.[35] In this case, y is the radial coordinate, with $y = 0$ at the centre of the cylinders. The shear stress in the flow is distributed according to

$$s = s_R \left(\frac{R}{y}\right)^2, \tag{31}$$

where s_R is the value of the shear stress at the surface of the inner cylinder; while the pressure p is essentially constant.[35] We assume that the volume fraction is everywhere larger than ν_c. This is the case when the tangential velocity of the inner cylinder U_R is less than a certain value U_M.[35] The numerical simulations indicate that s_R is independent of the angular velocity of the inner cylinder, so $s_R = s_M$, and the ratio s_M/p is equal to the value η in simple shearing.[35] With the stress ratio given by eqn (15) and (30), we obtain

$$I = \frac{1}{\left(p/\rho_p\right)^{1/2}} \frac{5\pi^{1/2}(1+e) s_M}{4J} \left(\frac{R}{y}\right)^2 T_R^{1/2} \exp\left(-\frac{y-R}{2\lambda}\right), \tag{32}$$

where $I = d|u'|/(p/\rho_p)^{1/2}$ is the so called inertial parameter.[49]

We assume that the slip velocity of the particles at the surface of the inner cylinder is proportional to the square root of the granular temperature, as is the case for collisional flows over bumpy walls.[41] Then, $U_R/U_M = (T_R/T_M)^{1/2}$ and eqn (32) can be written as

$$\frac{I}{I_M} = \frac{U_R}{U_M} \left(\frac{R}{y}\right)^2 \exp\left(-\frac{y-R}{2\lambda}\right), \tag{33}$$

where

$$I_M = \frac{5\pi^{1/2}(1+e) s_M}{4J} \frac{T_M^{1/2}}{p \left(p/\rho_p\right)^{1/2}} \tag{34}$$

is the value of the inertial parameter at the surface of the inner cylinder when $U_R = U_M$. When $U_R = U_M$, the granular temperature at $y = R$ is T_M, and, from eqn (13), has the value

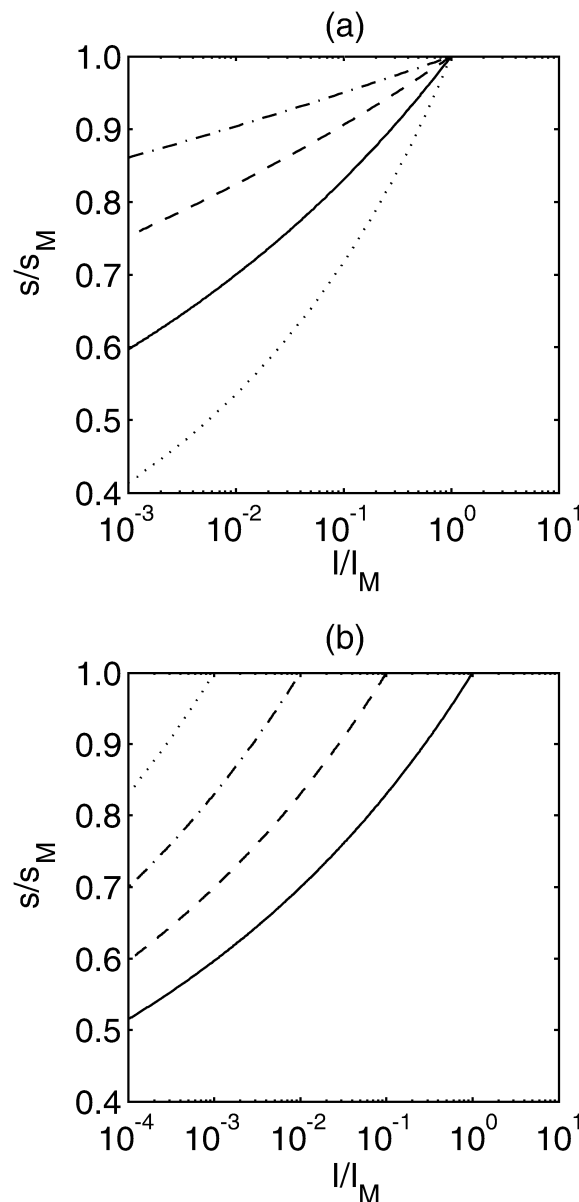$$T_M = \frac{144 p^2}{25\pi\nu_c^2(1+e)^2 \rho_p E}. \tag{35}$$

Fig. 6 Normalized stress ratio versus normalized inertial parameter in an annular shear cell for $e = 0.7$ and $\mu = 0.5$ and: (a) $U_R/U_M = 1$ and $R = 25$ (dotted line), $R = 50$ (solid line), $R = 100$ (dashed line) and $R = 200$ (dot-dashed line); (b) $R = 50$ and $U_R/U_M = 1$ (solid line), $U_R/U_M = 0.1$ (dashed line), $U_R/U_M = 0.01$ (dot-dashed line) and $U_R/U_M = 0.001$ (dotted line).

If the value of R is changed at constant angular velocity, with $U_R = U_M$, $e = 0.7$ and $\mu = 0.5$, we may employ eqn (31) and (33) to obtain the curves shown in Fig. 6a. If R is kept constant and the ratio U_R/U_M is changed at constant pressure, we obtain the curves of Fig. 6b. The quantities s/s_M and I/I_M are the shear stress and the inertial parameter, normalized by their respective values at the inner cylinder. These are in qualitative agreement with the results of the numerical simulations of Koval et al.,[35] shown in their Fig. 8b and 10. In both cases, the ratio s/s_M, is less than unity; that is, the ratio of the shear stress to the pressure is less than the yield stress ratio in simple shearing.

Conclusions

We have proposed constitutive relations for the steady, shearing flows of deformable, inelastic spheres that extend kinetic theories of granular gases to incorporate correlated, non-instantaneous collisions and rate-independent, elastic stresses. The latter are associated with the development of persistent deformations of the particles at volume fractions larger than a critical. The deformability of the particles plays a crucial role in the model. It permits a smooth transition between the collisional and deformational regimes and results in stress components in the deformational regime that contain both static contributions from particle elasticity and dynamic contributions from the momentum transfer associated with the release of elastic energy by the breaking of force chains.

The theory has been tested against previous numerical simulations of steady, homogeneous shearing of inelastic, frictional spheres that interact through linear elastic contacts with stiffnesses that range over eleven orders of magnitude. The theory also has the capacity to reproduce the exponentially decaying velocity profile in erodible beds and the dependence of the velocity on the radius and the angular velocity of the inner cylinder in annular shear flows. Although the constitutive relations have been developed for dry granular flows with inertial and frictional-elastic interactions, they are also relevant to the description of shear thickening in dense suspensions.[50,51] In such systems, a rapid increase in viscosity accompanies the jamming of frictional particles. For the slow shearing of compliant, frictional spheres, we anticipate that constitutive relations similar to those derived here, with the inertial interactions replaced by viscous interactions at volume fractions less than the critical, will predict the increases in viscosity seen in the numerical simulations and physical experiments.[52]

A final remark concerns the dependence of the viscosity – ratio of the shear stress to the shear rate – on the granular temperature predicted by the theory. When shearing takes place at a volume fraction below the critical, eqn (4) shows that the viscosity is proportional to $T^{1/2}$; that is, it increases with the granular temperature. This is the dependence of the molecular viscosity on the thermodynamic temperature seen in molecular gases. On the contrary, when shearing takes place at a volume fraction above the critical, eqn (13) through (15) show that the viscosity is inversely proportional to $T^{1/2}$; that is, it decreases with the granular temperature. This is the dependence of the molecular viscosity on the thermodynamic temperature seen in liquids. Interestingly, statistical physics models for the viscosity in liquids introduce a potential energy to predict the decrease of the viscosity with the temperature.[53] Here, we have obtained a similar result by means of mechanical arguments. Therefore, at least with respect to the dependence of the viscosity on the temperature, the critical volume fraction distinguishes between granular gases and granular liquids.

Acknowledgements

Notes and references

1 E. Irani, P. Chaudhuri and C. Heussinger, *Phys. Rev. Lett.*, 2014, **112**, 188303.
2 R. Piazza, *Rep. Prog. Phys.*, 2014, **77**, 056602.
3 J. Jenkins and S. Savage, *J. Fluid Mech.*, 1983, **130**, 187–202.
4 V. Garzó and J. W. Dufty, *Phys. Rev. E: Stat. Phys., Plasmas, Fluids, Relat. Interdiscip. Top.*, 1999, **59**, 5895–5911.
5 I. Goldhirsch, *Annu. Rev. Fluid Mech.*, 2003, **35**, 267–293.
6 E. Azanza, F. Chevoir and P. Moucheront, *J. Fluid Mech.*, 1999, **400**, 199–227.
7 Y. Forterre and O. Pouliquen, *Phys. Rev. Lett.*, 2001, **86**, 5886.
8 H. Xu, M. Louge and A. Reeves, *Continuum Mech. Thermodyn.*, 2003, **15**, 321–349.
9 J. T. Jenkins, *Phys. Fluids*, 2006, **18**, 103307.
10 S. Torquato, *Phys. Rev. E: Stat. Phys., Plasmas, Fluids, Relat. Interdiscip. Top.*, 1995, **51**, 3170–3182.
11 N. Mitarai and H. Nakanishi, *Phys. Rev. Lett.*, 2005, **94**, 128001.
12 N. Mitarai and H. Nakanishi, *Phys. Rev. E: Stat., Nonlinear, Soft Matter Phys.*, 2007, **75**, 031305.
13 V. Kumaran, *J. Fluid Mech.*, 2009, **632**, 145–198.
14 J. T. Jenkins, *Granular Matter*, 2007, **10**, 47–52.
15 J. T. Jenkins and D. Berzi, *Granular Matter*, 2010, **12**, 151–158.
16 D. Berzi, *Acta Mech.*, 2014, **225**, 2191–2198.
17 D. Berzi and J. T. Jenkins, *Phys. Fluids*, 2011, **23**, 013303.
18 J. T. Jenkins and D. Berzi, *Granular Matter*, 2012, **14**, 79–84.
19 D. Vescovi, D. Berzi, P. Richard and N. Brodu, *Phys. Fluids*, 2014, **26**, 053305.
20 D. Berzi and D. Vescovi, *Phys. Fluids*, 2015, **27**, 013302.
21 S. Chialvo, J. Sun and S. Sundaresan, *Phys. Rev. E: Stat., Nonlinear, Soft Matter Phys.*, 2012, **85**, 021305.
22 A. J. Liu and S. R. Nagel, *Annu. Rev. Condens. Matter Phys.*, 2010, **1**, 347–369.
23 C. Heussinger, P. Chaudhuri and J.-L. Barrat, *Soft Matter*, 2010, **6**, 3050–3058.
24 M. van Hecke, *J. Phys.: Condens. Matter*, 2010, **22**, 033101.
25 L. E. Silbert, *Soft Matter*, 2010, **6**, 2918.
26 M. Otsuki, H. Hayakawa and S. Luding, *Prog. Theor. Phys. Suppl.*, 2010, **184**, 110–133.
27 M. P. Ciamarra, R. Pastore, M. Nicodemi and A. Coniglio, *Phys. Rev. E: Stat., Nonlinear, Soft Matter Phys.*, 2011, **84**, 1–10.
28 M. Grob, C. Heussinger and A. Zippelius, *Phys. Rev. E: Stat., Nonlinear, Soft Matter Phys.*, 2014, **89**, 2–5.
29 J. Sun and S. Sundaresan, *J. Fluid Mech.*, 2011, **682**, 590–616.
30 H. Hwang and K. Hutter, *Continuum Mech. Thermodyn.*, 1995, **7**, 357–384.
31 P. Johnson, P. Nott and R. Jackson, *J. Fluid Mech.*, 1990, **210**, 501–535.
32 D. Berzi, C. di Prisco and D. Vescovi, *Phys. Rev. E: Stat., Nonlinear, Soft Matter Phys.*, 2011, **84**, 1–6.
33 S. Ji and H. H. Shen, *J. Rheol.*, 2008, **52**, 87–103.
34 S. Chialvo and S. Sundaresan, *Phys. Fluids*, 2013, **25**, 070603.
35 G. Koval, J.-N. Roux, A. Corfdir and F. Chevoir, *Phys. Rev. E: Stat., Nonlinear, Soft Matter Phys.*, 2009, **79**, 021306.

36 S. Chapman and T. G. Cowling, *The mathematical theory of non-uniform gases*, Cambridge University Press, 3rd edition, 1970.

37 C. S. Campbell, *J. Fluid Mech.*, 2002, **465**, 261–291.

38 D. Berzi and J. T. Jenkins, *Phys. Fluids*, 2015, **27**, 113303.

39 J. T. Jenkins and C. Zhang, *Phys. Fluids*, 2002, **14**, 1228.

40 M. Larcher and J. T. Jenkins, *Phys. Fluids*, 2013, **25**, 113301.

41 M. W. Richman, *Acta Mech.*, 1988, **75**, 227–240.

42 J. T. Jenkins and E. Askari, *J. Fluid Mech.*, 1991, **223**, 497–508.

43 J. T. Jenkins and O. D. L. Strack, *Mech. Mater.*, 1993, **16**, 25–33.

44 D. Howell, R. Behringer and C. Veje, *Phys. Rev. Lett.*, 1999, **82**, 5241–5244.

45 L. D. Landau and E. M. Lifschitz, *Theory of elasticity*, 1959.

46 S. F. Foerster, M. Y. Louge, H. Chang and K. Allia, *Phys. Fluids*, 1994, **6**, 1108.

47 T. Komatsu, S. Inagaki, N. Nakagawa and S. Nasuno, *Phys. Rev. Lett.*, 2001, **86**, 1757–1760.

48 K. Kamrin and G. Koval, *Phys. Rev. Lett.*, 2012, **108**, 178301.

49 G. D. R. Midi, *Eur. Phys. J. E: Soft Matter Biol. Phys.*, 2004, **14**, 341–365.

50 R. Seto, R. Mari, J. F. Morris and M. M. Denn, *Phys. Rev. Lett.*, 2013, **111**, 1–5.

51 C. Heussinger, *Phys. Rev. E: Stat., Nonlinear, Soft Matter Phys.*, 2013, **88**, 050201.

52 E. Brown and H. M. Jaeger, *J. Rheol.*, 2012, **56**, 875.

53 H. Eyring and J. Hirschfelder, *J. Phys. Chem.*, 1937, **41**, 249–257.